Atmos. Chem. Phys. Discuss., 3, 4069–4096, 2003
www.atmos-chem-phys.org/acpd/3/4069/

Atmospheric Chemistry and Physics Discussions

DRIFTS and Knudsen cell study of the heterogeneous reactivity of SO_2 and NO_2 on mineral dust

M. Ullerstam[1], **M. S. Johnson**[2], **R. Vogt**[3], **and E. Ljungström**[1]

[1]Gothenburg University, Department of Chemistry, SE-41296 Gothenburg, Sweden
[2]Copenhagen University, Department of Chemistry, Universitetsparken 5, DK-2100 Copenhagen Ø, Denmark
[3]Ford Forschungszentrum GmbH Aachen, Süsterfeldstrasse 200, D-52072 Aachen, Germany

Received: 14 July 2003 – Accepted: 3 June 2003 – Published: 28 July 2003

Correspondence to: M. Ullerstam (mariau@inoc.gu.se)

Abstract

The heterogeneous oxidation of SO_2 by NO_2 on mineral dust was studied using Diffuse Reflectance Infrared Fourier Transform Spectroscopy (DRIFTS) and a Knudsen cell. This made it possible to characterise, kinetically, both the formation of sulfate and nitrate as surface products and the gas phase loss of the reactive species. The gas phase loss rate was determined to be first order in both SO_2 and NO_2. From the DRIFTS experiment the uptake coefficient, γ, for the formation of sulfate was determined to be of the order of 10^{-10} using the BET area as the reactive surface area. No significant formation of sulfate was seen in the absence of NO_2. The Knudsen cell study gave uptake coefficients of the order of 10^{-6} and 10^{-7} for SO_2 and NO_2, respectively. There was no significant difference in uptake when SO_2 or NO_2 were introduced individually compared to experiments in which SO_2 and NO_2 were present at the same time.

1. Introduction

Particulate matter present in the Earth's atmosphere provides reactive surfaces for heterogeneous chemistry. A large contribution to the tropospheric aerosol budget is mineral aerosol that originates from arid and semi-arid areas. The annual flux of mineral aerosol to the atmosphere is estimated to be between 1000 and 3000 Tg, and with changes in precipitation patterns and land use, the emissions of mineral aerosol may increase substantially which would increase their importance in the atmosphere (Dentener et al., 1996; Tegen and Fung, 1994; Zhang and Carmichael, 1999). Atmospheric aerosol particles are known to affect radiative transfer by scattering and absorbing light and they can also influence the optical properties of clouds. Understanding interactions between the gas and the condensed phase is important because these processes may influence the photochemical oxidation capacity of the atmosphere as well as changing aerosol composition and size distribution (Dentener et al., 1996; Galy-Lacaux et al.,

ACPD

3, 4069–4096, 2003

2001; Martin et al., 2003; Zhang and Carmichael, 1999). Recent modeling work has shown how aerosols modify the chemical properties of the atmosphere, decreasing the photolysis rate of ozone and the concentration of HO_x, increasing the concentration of CO, and producing HNO_3 from NO_2 and NO_3 (Martin et al., 2003).

Field measurements of the chemical composition of aerosol particles in East Asia show strong correlations between nitrate and non-sea-salt calcium (i.e. the mineral aerosol fraction) (Carmichael et al., 1996; Nishikawa et al., 1991; Zhang et al., 2000). Such a correlation, while not as strong, is also seen for non-sea-salt sulfate and mineral aerosol (Carmichael et al., 1996; Niahikawa et al., 1991; Zhang et al., 2000). The observed correlations could be caused by surface reactions of sulfur and nitrogen species. An indication that particles originating from soil are more likely to contain a mixture of sulfate and nitrate than other kinds of particles has also been found (Zhang et al., 2000).

However, large uncertainties remain concerning the effect of chemical composition and surface properties on heterogeneous reaction kinetics.

In the present study, the heterogeneous reaction of SO_2 and NO_2 on mineral dust was investigated using the Knudsen cell and Diffuse Reflectance Infrared Fourier Transform Spectroscopy (DRIFTS) techniques. Mineral dust samples from the Cape Verde Islands, located off Mauritania and Senegal on the west coast of Africa, were used for the experiments. The mineral dust consists of a $< 20\,\mu$m diameter fraction and has a BET surface area of $5 \times 10^5\,cm^2\,g^{-1}$. The samples are representative of mineral dust from the Saharan desert and the main content of the samples is quartz and potassium feldspars (Desboeufs et al., 1999; Rognon et al., 1996).

ACPD
3, 4069–4096, 2003

2. Experimental

2.1. Knudsen cell experiments

A Knudsen cell was used for the analysis of loss from the gas phase due to surface reactions or adsorption. The Knudsen cell reactor consists of a chamber with an isolated sample compartment and a small orifice through which gas phase reactant and product species can escape to be detected by mass spectrometry. To assure molecular flow, the mean free path must be at least a factor of 10 greater than the diameter of the exit orifice, which was maintained by a low pressure in the cell (Golden et al., 1973). The Knudsen reactor setup has previously been described (Monster et al., 2002). The reaction chamber is a 6-way ISO 100 cross sealed with Viton O-rings, which is connected to a quadrupole mass spectrometer (Leda Mass). Inside the reactor a plunger makes it possible to either cover or expose the sample holder. To minimize wall reactions the reactor walls were passivated with a coating of Teflon. The temperature of the sample holder can be controlled from 233 to 373 K using a Peltier cooler and a cryofluid pump. The design of the gas system makes it possible to introduce the reactive gases in two ways, either through a pulsed valve or as a continuous flow through needle valves. The pulsed valve is a solenoid valve (General Valve P/N 009-1562-900) with a 0.8 millimetre orifice, and can generate pulses from a few hundred microseconds to several hours at a repetition rate of up to 2500 Hz. The use of a pulsed valve in combination with a Knudsen cell was first described by Tabor et al. (1994). The system uses a dual needle valve (Nupro) to regulate the gas flow in the steady state mode.

The dust samples were applied to the sample holder using an atomizer containing a water suspension of the mineral dust. The aerosol is sprayed onto the sample holder which was preheated to 373 K. This procedure enables the formation of a thin uniform surface of the mineral dust. The sample was kept in the evacuated reaction chamber at 333 K for 1h prior to experiments. This treatment has been shown to give a reproducible reactivity, and removes excess water from the sample (Ullerstam et al., 2002). After the system was cooled to room temperature the plunger was lowered and the sample was

covered. A fresh mixture of the reactive gases with known concentration was made before every experiment and was introduced into the chamber either as a pulse or as a steady state flow. Parameters for the Knudsen reaction chamber can be found in Table 1.

NO_2 (>98%, Hede Nielsen) and SO_2 (99.9%, Gerling Holtz and Company) were used for the Knudsen cell experiments.

2.2. Experiments using the DRIFTS technique

The DRIFTS technique was used to analyse the surface reactions. Infrared spectra were recorded in the spectral range from 4000 to 600 cm^{-1} with a Bruker Equinox 55 FTIR spectrometer equipped with a mercury cadmium telluride (MCT) detector and DRIFTS optics (model DRA-2CO, Harrick Scientific Corp.). General features of the setup have previously been described (Borensen et al., 2000; Ullerstam et al., 2002). Spectra were recorded at a resolution of 4 cm^{-1} and 100 scans were averaged for each spectrum resulting in a time resolution of 1 min. The dust samples were prepared as a water suspension on glass plates, with dimensions of 9 × 9 mm^2 followed by drying in an oven (10 min, 333 K). The reaction chamber was flushed with He carrier gas while the sample was kept at 333 K for 1 h at a pressure of 4.5 mbar before an experiment was started. Spectra were collected as difference spectra with the unreacted dust as the background, thus surface products appear as positive bands while losses of surface species give rise to negative bands. Surface reactants were quantified by ion chromatography using a Dionex DX 120 system, equipped with a Dionex AS 14 analytical column and a conductivity detector (CD 20) with detection stabilizer. A more detailed description of the analysis is available (Ullerstam et al., 2002).

NO_2 for the DRIFTS experiments was synthesized from the reaction between NO (>99.5%, Messer-Griesheim) and O_2 (>99.998%, Messer-Griesheim). SO_2 (>99.98%, Messer-Griesheim) was diluted with He before use.

ACPD
3, 4069–4096, 2003

3. Results

3.1. Observed products

The unexposed dust sample is used to collect a background spectrum and therefore both positive and negative features were observed in the subsequent spectra. Investigations were made in which mineral dust was reacted just with NO_2, or with SO_2 and NO_2 simultaneously using the DRIFTS technique. When only NO_2 was added a number of absorption bands were observed, as can be seen in Fig. 1a. The most prominent positive features are two bands between 1500 and 1300 cm^{-1} which can be assigned to the degenerate asymmetric stretch vibration of the nitrate ion (Borensen et al., 2000; Hadjiivanov et al., 1994; Nakamoto, 1997; Underwood et al., 1999). The splitting of the ν_3 vibration is due to an interaction with the surface, resulting in a reduced symmetry for the nitrate species. The nitrate ion can coordinate to a metal as a unidentate, chelating bidentate or bridging bidentate ligand. It is difficult to distinguish between these possibilities since the symmetry differs very little (Nakamoto, 1997). At lower wavenumbers at the end of the nitrate band at 1250 cm^{-1} there is a smaller positive band that may be assigned to the asymmetric stretch of nitrite (Borensen et al., 2000; Hadjiivanov et al., 1994). Both nitrate and nitrite ions are found in the ion chromatography analysis. A small negative band is also present at 1650 cm^{-1} indicating loss of surface species originating from surface-adsorbed water (Nakamoto, 1997). This loss of water during the reaction is also seen as a negative band in the area around 3200 cm^{-1}. The loss of different types of free OH groups at the surface is evidenced as a small negative band at 3700 cm^{-1} (not shown in figure) (Tsyganenko and Mardilovich, 1996). When SO_2 is introduced simultaneously with NO_2 the bands of nitrate are still dominant, especially when the ratio of SO_2 to NO_2 is low, cf. Fig. 1b. However at higher ratios the bands of sulfur species become evident. The small narrow band at 1330 cm^{-1} on the top of the broader nitrate band is due to physisorbed SO_2 (Chang, 1978; Datta et al., 1985; Deo and Dalla Lana, 1971; Goodman et al., 2001; Nakamoto, 1997; Ullerstam et al., 2002). The nitrate band is also to some extent distorted and the nitrite band is superimposed

ACPD
3, 4069–4096, 2003

on the band of surface bound sulfate at 1240 cm^{-1} (Meyer et al., 1980; Schoonheydt and Lunsford, 1972; Ullerstam et al., 2002; Usher et al., 2002). The loss of free OH groups is larger when SO_2 is present which indicates that SO_2 is adsorbed to these free OH groups while NO_2 may adsorb on other reactive sites as well. A broad band at 2450 cm^{-1} during exposure to SO_2 also indicates some formation of hydrogen sulfite (Meyer et al., 1980; Nakamoto, 1997). Subtraction of the nitrate features in the spectra derived from experiments with both SO_2 and NO_2 present, using the pure NO_2 experiment as a reference, results in a spectrum with a band around 1280 cm^{-1} (Fig. 1c) which is assigned to the sulfate band although shifted 40 cm^{-1} relative to the band of surface bound sulfate. The peak at 1330 cm^{-1} is due to physisorbed SO_2 which is not subtracted. A similar procedure was made to subtract the sulfate band revealing the nitrate features between 1500 and 1300 cm^{-1} which can be seen in Fig. 2c. The reference spectra (a) in Fig. 2 with features of physisorbed SO_2 and SO_4^{2-} were obtained from an earlier experiment with the same substrate (Ullerstam et al., 2002). Weak features below 1000 cm^{-1} may not be detectable due to the low signal-to-noise ratio in this region.

3.2. Kinetics, Knudsen cell

The total uptake coefficient (γ_{total}) is defined as the fraction of collisions with the surface that results in loss of the molecule from the gas phase divided by the total number of surface collisions per unit time. From the Knudsen experiments this can be calculated from the first order rate constant of the uptake (k_f), the collision frequency (Z) and the reactive surface area (A_s).

$$\gamma_{total} = \frac{k_f}{Z \times A_s} \quad (1)$$

$$Z = \sqrt{\frac{8 \times R \times T}{\pi \times M}} \times \frac{1}{4V}, \quad (2)$$

where R is the gas constant (J mol^{-1} K^{-1}), T is the temperature (K) and V is the volume of the reactor (m^3).

The data treatment of the first order rate constant (k_f) depends on whether the reactive gases are introduced as a pulse or as a steady state flow. In an experiment with pulsed flow the decay rate is measured with and without the sample covered. The decay is equal to the lifetime of the gas in the chamber which is the inverse of the loss rate, $k = 1/\tau$. Experiments are performed with the sample holder covered or open.

$$k_{Kc} = k_e \tag{3}$$

$$k_{Kc+s} = k_e + k_u. \tag{4}$$

Here Kc signifies Knudsen cell; e, escape: u, uptake and s, sample exposed. Rearranging gives,

$$k_u = k_{Kc} + sk_{Kc}. \tag{5}$$

Thus k_u in Eq. (5) is equal to the first order rate (k_f) in Eq. (1) and no knowledge of the theoretical value of k_e is necessary. The value k_e is the theoretical escape rate for the specific gas and aperture.

$$k_e = Z \times A_h, \tag{6}$$

where A_h is the area of the escape aperture, corrected for the limitation to the flow caused by the nonzero length of the aperture.

For a steady state flow experiment, the first order rate is obtained by measuring the relative intensity of the signal before (S_0) and during (S_R) the exposure of the sample according to Eq. (7).

$$k_f = k_e \left(\frac{S_0}{S_R} - 1 \right). \tag{7}$$

To study the dependence of the uptake coefficient on sample mass, using the geometric area (projected surface) as the effective surface area, a number of experiments with

ACPD
3, 4069–4096, 2003

different sample mass but constant concentration of SO_2 and NO_2 were performed; the results are shown in Fig. 3. This was done to ensure that experiments were conducted in the linear mass regime where the entire sample participates in the reaction and the BET surface area can be used as the reactive surface area (Grassian, 2002; Underwood et al., 2000). These experiments were made with a pulsed flow where each pulse contained 2.7×10^{11} and 1.7×10^{11} molecules of SO_2 and NO_2, respectively. An example of a typical experiment is shown in Fig. 4. The resulting uptake coefficient for SO_2 was determined to be $(1.6 \pm 0.1) \times 10^{-5}$ using the BET area as the reactive surface area.

A number of experiments were carried out using a constant concentration of NO_2 while the concentration of SO_2 was varied, to study the uptake coefficient of SO_2 in the presence of NO_2. Another set of experiments was made with different concentrations of NO_2 but constant concentration of SO_2 to obtain the uptake coefficient of NO_2 in the presence of SO_2. A typical experiment is shown in Fig. 5. All the experiments were made with a steady state flow of the reactive gases and the sample mass was kept at around 20 mg of mineral dust to maintain "linear mass" conditions. A summary of the results can be found in Table 2. The errors are reported at the 95% confidence interval, as determined from the standard deviation of an ensemble of experiments. It can be seen that the results from the steady state experiment give an uptake coefficient that is around 3 times smaller relative to the pulsed experiments. The discrepancy may be caused by the lower time resolution of a steady state experiment. In a steady state experiment, the true initial uptake coefficient may be hidden because of the time required to lift the sample cover (Monster et al., 2002).

The observed relative loss of SO_2 and NO_2 from the gas phase during the experiments was 63 ± 10 and 18 ± 5%, respectively. A log-log plot of the initial loss rate of SO_2 versus the concentration of SO_2 shown in Fig. 6, gives a slope of 1.02 ± 0.24 (2σ) i.e. the SO_2 loss has an apparent first order dependence on $[SO_2]$. An equivalent plot was made for NO_2 which gave a slope of 0.86×0.18 (2σ) which also indicates a reaction order of 1 for NO_2 which is shown in Fig. 7. This means that in both cases

the adsorption rate depends on the concentration of the reactive species and that the uptake coefficient is independent of concentration.

3.3. Kinetics, DRIFTS

The amount of sulfate on the sample was determined by ion chromatography in order to quantify the sulfate formation rate $d\left[SO_4^{2-}\right]/dt$ in terms of the reactive uptake coefficient. The initial formation rate was translated from absorption units s^{-1} to SO_4^{2-} s^{-1} by a conversion factor obtained from a calibration plot. Since the absorption bands of the different reaction product species overlap one another, the bands are deconvoluted before integration. The reactive uptake coefficient (γ_{rxn}) is defined as the number of reactive collisions with the surface ($d\left[SO_4^{-2}\right]/dt$) divided by the total number of surface collisions per unit time (Ω).

$$\gamma_{rxn} = \frac{d\left[SO_4^{-2}\right]/dt}{\Omega} \tag{8}$$

$$\Omega = \frac{1}{4} \times A_s \times [SO_2] \times \nu_{SO_2}, \tag{9}$$

where ν is the mean molecular velocity of SO_2 calculated as $\sqrt{8RT/\pi M_{SO_2}}$ and A_s is the effective sample surface. $d\left[SO_4^{2-}\right]/dt$ was obtained from the absorbance/time plot at t_0 i.e. the initial rate, thus no saturation effects on γ are expected.

A sequence of experiments was performed with a constant concentration of NO_2 and varying concentrations of SO_2. The results can be seen in Table 2. The observed relative loss from the gas phase resulting in reactive species on the surface was between 1.5% to 7.8% and 0.15% to 0.57% for SO_2 and NO_2, respectively. The experiments that were terminated at a short reaction time were the ones with largest relative loss from the gas phase. This is expected since the loss rate of reactive species is fast in

ACPD
3, 4069–4096, 2003

the initial phase of the experiment but decreases with increasing exposure due to the loss of reactive sites on the surface.

The introduction of SO_2 to the reactive gas reduces the formation of surface nitrate species compared to experiment with only NO_2. From the ion chromatography analysis at the end of the experiment in which only NO_2 was introduced, the total amount of surface nitrate was 2.1×10^{16} ions ($[NO_2] = 2.2 \times 10^{13}$ molecule cm^{-3}, reaction time = 160 min). A similar experiment in which SO_2 also was present only produced 7.6×10^{15} ions of surface nitrate species, which corresponds to a reduction by almost 40% ($[NO_2] = 2.1 \times 10^{13}$ molecule cm^{-3}, $[SO_2] = 2.4 \times 10^{12}$ molecule cm^{-3} and reaction time = 150 min).

3.4. Mechanism

The reaction of NO_2 with surface adsorbed water is well-known and has been shown to be first order in NO_2 (Jenkin et al., 1988; Kleffmann et al., 1998; Langer et al., 1997; Mertes and Wahner, 1995; Pitts et al., 1984; Sakamaki et al., 1983; Svensson et al., 1987).

$$2NO_{2(g)} + H_2O_{(ads)} \longrightarrow HONO_{(g)} + HNO_{3(ads)}. \quad \text{(R1)}$$

In this study the experiments were performed under "dry" conditions. However, some adsorbed water will be present in the dust sample, since the samples were only heated to 333 K prior to exposure. Different types of water-related reactive sites are present on the surface in the form of O^- or OH groups.

A previous study of the uptake of SO_2 proposed a two step mechanism for the oxidation of SO_2 where the first step is a reversible adsorption of SO_2 onto the surface followed by a second, irreversible reaction in which adsorbed SO_2 is oxidized to sulfate (Ullerstam et al., 2002).

$$^*OH + SO_{2(g)} \longleftrightarrow *OH \cdots SO_{2(ads)}, \quad \text{(R2)}$$

were *OH denotes free surface OH groups.

ACPD
3, 4069–4096, 2003

In the present investigation the oxidant is gaseous NO_2 which reacts with the surface adsorbed SO_2 forming surface sulfate and NO which escapes to the gas phase.

$$^{*}OH \cdots SO_{2(ads)} + NO_{2(g)} \rightarrow^{*} OHSO^{-}_{3(ads)} + NO_{(g)}. \quad \text{(R3)}$$

There would appear to be a competition for NO_2, between surface adsorption forming nitrate, and its acting as an oxidant, forming sulfate (i.e. reaction (R1) vs. (R3)). The oxidation is not fast enough to be the only process on the surface: the surface formation of nitrates is also taking place. This is also indicated by the reduction of surface nitrate products from the experiments in which both reactive gases are present compared, to experiments with only NO_2 exposure.

4. Discussion and conclusions

The uptake coefficients for SO_2 in the presence of NO_2 measured using the two different techniques differ by a factor of around 10^3 and 2×10^4 ("geometric" and BET ratios, respectively), where the DRIFTS technique produces the lower results. This cannot only be accounted for by the lower time resolution of the DRIFTS technique. The uptake coefficients obtained using the two techniques are fundamentally different. The Knudsen cell measures the loss of gaseous species during exposure, while the DRIFTS technique determines the rate of formation of products on the surface. The discrepancy between the results can be explained by the equilibrium between species physisorbed on the surface and those found in the gas phase. The higher relative loss of gaseous SO_2 and NO_2 from the Knudsen cell experiments compared to the DRIFTS experiments support this. In the Knudsen experiments there is no difference between the uptake coefficients measured using pure SO_2 or NO_2, and the uptake coefficient measured in experiments with both reactive gases present. In the case of uptake of SO_2 this is likely because the rate of physisorption is faster than the rate of sulfate formation and thus the uptake coefficient is determined by the rate of physisorption.

There have been a number of studies concerning the uptake of NO_2 and SO_2 on different surfaces or materials. Very often substances that are components of crustal material are used, such as Al_2O_3, Fe_2O_3, MgO, and SiO_2. There are also a few studies in which natural dust samples have been used. One such study investigated the uptake of NO_2 and reported uptake coefficients of the order of 10^{-6} on China Loess and Saharan sand (Underwood et al., 2001). An uptake coefficient for SO_2 on China Loess of the order of 10^{-5} has also been reported (Usher et al., 2002). This is a factor of ten higher that our result for both NO_2 and SO_2.

The SO_2 deposition velocity on limestone and sandstone in the presence of NO_2 has been reported with a maximum of 0.45 cm s^{-1} (Ausset et al., 1996). A rough estimate of the equivalent uptake coefficient from the deposition velocity can be made using the expression $\gamma = 4v_d/v_m$, were the v_d is the deposition velocity and v_m the molecular velocity (Dentener et al., 1996). The uptake coefficient is estimated to be 5×10^{-5}, which is also around a factor of ten higher than our result. It is clear that natural mineral samples with different compositions will have different reactivities.

The formation of surface sulfate is an important characteristic since it changes the physical properties of the mineral dust particle. A particle coated with sulfate is hygroscopic and will take up water; it may therefore take up more SO_2 into this aqueous layer that would otherwise be formed (Zhang and Chan, 2002). The formation of sulfate on mineral dust is thus a competing oxidation process for SO_2 in the atmosphere. This may affect the estimated cooling effect of sulfate aerosols since sulfate on mineral particles is not believed to change the radiative properties of those dust particles (Dentener et al., 1996).

To be able to compare the lifetime and the importance of heterogeneous reactions with other losses such as gas phase reactions the heterogeneous rates were translated to a pseudo-first order mass transfer constant as described by Li and co-workers (Li et

al., 2001).

$$K_j = \int_{r2}^{r1} 4\pi r^2 F(r) \frac{dn}{dr} dr \tag{10}$$

$$F(r) = \frac{D_j / r}{1 + f(K_n, \gamma) K_n} \tag{11}$$

$$f(K_n, \gamma) = \frac{1.333 + 0.71\, K_n^{-1}}{1 + K_n^{-1}} + \frac{4(1-\gamma)}{3\gamma}, \tag{12}$$

where k_j is the overall mass transfer coefficient, in $cm^3\ s^{-1}$, for species j; D_j is the gas phase diffusion coefficient in $cm^2\ s^{-1}$; K_n is the dimensionless Knudsen number ($= \lambda / r$), γ is the effective free path of a gas molecule in air; r is the particle radius; $F(r)$ is the flux of the trace species to the surface of the aerosol particle with radius r in molecule $cm\ s^{-1}$; dn/dr is the number-size distribution of aerosol particles, and γ is the uptake coefficient.

The mass transfer coefficient (k_j) was calculated from the above expressions as a function of uptake coefficient by using the lognormal distribution for the aerosol number-size distribution.

$$\frac{dn(r)}{d(\log r)} = \sum_{i=1}^{3} \frac{n_i}{\log\sigma_i \sqrt{2\pi}} \exp\left\{ \frac{-\left(\log r / R_i\right)^2}{2\left(\log\sigma_i\right)^2} \right\}, \tag{13}$$

where r is the particle radius in μm, $n(r)$ is the cumulative particle number distribution in cm^{-3} for particles larger than r, R is the mean particle radius in μm, n is the integral of the lognormal function, and $\log\sigma$ is a measure of particle polydispersity.

The corresponding lifetime is calculated as a function of γ as is shown in Fig. 8. The lifetime of SO_2 calculated from the reaction with OH radicals in the gas phase is

equal to 13 days (k = 8.8 × 10^{-13} cm^3 $molecule^{-1}$ s^{-1} and [OH] = 1 × 10^6 molecule cm^{-3}) (DeMore et al., 1997). From the plot it can be seen that this would correspond to a γ in the order of around 10^{-4}. The lifetime of NO_2 in the gas phase is even lower considering the reaction with OH radicals and O_3 which corresponds to 16 h and 3.5 h, respectively (k_{OH} = 8.8 × 10^{-12} and k_{O_3} = 3.2 × 10^{-17} in cm^3 $molecule^{-1}$ s^{-1}, [OH] = 1 × 10^6 and [O_3] = 2.5 × 10^{12} in molecule cm^{-3}). However, during episodes of high dust loading in the atmosphere, heterogeneous reactions are likely to be the dominant loss process for SO_2. In addition to the increased heterogeneous loss of SO_2 caused by increased dust surface area, loss of SO_2 by reaction with OH is suppressed. The OH concentrations will fall due to the absorption and scattering of sunlight by the dust.

Acknowledgements. We would like to thank T. Rosenørn and J. Mønster for help with the Knudsen cell. This work was supported by the Nordic Network for Chemical Kinetics funded by the Nordic Academy for Advanced Study, and the Danish Natural Sciences Research Council.

References

Ausset, P., Crovisier, J. L., delMonte, M., Furlan, V., Girardet, F., Hammecker, C., Jeannette, D. and Lefevre, R. A.: Experimental study of limestone and sandstone sulphation in polluted realistic conditions: The Lausanne Atmospheric Simulation Chamber (LASC), Atmospheric Environment, 30, 3197–3207, 1996.

Borensen, C., Kirchner, U., Scheer, V., Vogt, R., and Zellner, R.: Mechanism and kinetics of the reactions of NO_2 or HNO_3 with alumina as a mineral dust model compound, Journal of Physical Chemistry A, 104, 5036–5045, 2000.

Carmichael, G. R., Zhang, Y., Chen, L. L., Hong, M. S., and Ueda, H.: Seasonal variation of aerosol composition at Cheju Island, Korea, Atmospheric Environment, 30, 2407–2416, 1996.

Chang, C. C.: Infrared Studies of SO_2 on Gamma-Alumina, Journal of Catalysis, 53, 374–385, 1978.

Datta, A., Cavell, R. G., Tower, R. W. and George, Z. M.: Claus Catalysis .1. Adsorption of

SO_2 on the Alumina Catalyst Studied by Ftir and Electron-Paramagnetic-Res Spectroscopy, Journal of Physical Chemistry, 89, 443–449, 1985.
Dentener, F. J., Carmichael, G. R., Zhang, Y., Lelieveld, J., and Crutzen, P. J.: Role of mineral aerosol as a reactive surface in the global troposphere, Journal of Geophysical Research Atmospheres, 101, 22 869–22 889, 1996.
Deo, A. V. and Dalla Lana, I. G.: Infrared studies of the adsorption and surface reactions of hydrogen sulfide and sulfur dioxide on some aluminas and zeolites, Journal of Catalysis, 21, 270–281, 1971.
Desboeufs, K. V., Losno, R., Vimeux, F., and Cholbi, S.: The pH-dependent dissolution of wind-transported Saharan dust, Journal of Geophysical Research-Atmospheres, 104, 21 287–21 299, 1999.
Galy-Lacaux, C., Carmichael, G. R., Song, C. H., Lacaux, J. P., Al Ourabi, H., and Modi, A. I.: Heterogeneous processes involving nitrogenous compounds and Saharan dust inferred from measurements and model calculations, Journal of Geophysical Research Atmospheres, 106, 12 559–12 578, 2001.
Golden, D. M., Spokes, G. N., and Benson, S. W.: Pyrolyse bei sehr kleinem Druck (VLPP); eine vielseitige kinetische Methode, Angewandte Chemie, 85, 602–614, 1973.
Goodman, A. L., Li, P., Usher, C. R., and Grassian, V. H.: Heterogeneous uptake of sulfur dioxide on aluminum and magnesium oxide particles, Journal of Physical Chemistry A, 105, 6109–6120, 2001.
Grassian, V. H.: Chemical reactions of nitrogen oxides on the surface of oxide, carbonate, soot, and mineral dust particles: Implications for the chemical balance of the troposphere, Journal of Physical Chemistry A, 106, 860–877, 2002.
Hadjiivanov, K., Bushev, V., Kantcheva, M., and Klissurski, D.: Infrared-Spectroscopy Study of the Species Arising During NO_2 Adsorption on TiO_2 (Anatase), Langmuir, 10, 464–471, 1994.
Jenkin, M. E., Cox, R. A., and Williams, D. J.: Laboratory studies of the kinetics of formation of nitrous acid from the thermal reaction of nitrogen dioxide and water vapour, Atmospheric Environment, 22, 487–498, 1988.
Kleffmann, J., Becker, K. H., and Wiesen, P.: Heterogeneous NO_2 conversion processes on acid surfaces: Possible atmospheric implications, Atmospheric Environment, 32, 2721–2729, 1998.
Langer, S., Pemberton, R. S., and FinlaysonPitts, B. J.: Diffuse reflectance infrared studies of

the reaction of synthetic sea salt mixtures with NO_2: A key role for hydrates in the kinetics and mechanism, Journal of Physical Chemistry A, 101, 1277–1286, 1997.

Li, P., Perreau, K. A., Covington, E., Song, C. H., Carmichael, G. R., and Grassian, V. H.: Heterogeneous reactions of volatile organic compounds on oxide particles of the most abundant crustal elements: Surface reactions of acetaldehyde, acetone, and propionaldehyde on SiO_2, Al_2O_3, Fe_2O_3, TiO_2, and CaO, Journal of Geophysical Research Atmospheres, 106, 5517–5529, 2001.

Martin, R. V., Jacob, D. J., Yantosca, R. M., Chin, M., and Ginoux, P.: Global and regional decreases in tropospheric oxidants from photochemical effects of aerosols, Journal of Geophysical Research Atmospheres, 108, 4097–4115, 2003.

Mertes, S. and Wahner, A.: Uptake of Nitrogen-Dioxide and Nitrous-Acid on Aqueous Surfaces, Journal of Physical Chemistry, 99, 14 000–14 006, 1995.

Meyer, B., Ospina, M., and Peter, L. B.: Raman Spectrometric Determination of Oxysulfur Anions in Aqueous Systems, Analytica Chimica Acta, 117, 301–311, 1980.

Monster, J., Rosenorn, T., Nielsen, O. J., and Johnson, M. S.: Knudsen cell construction, validation and studies of the uptake of oxygenated fuel additives on soot, Environmental Science & Pollution Research, Special Issue 1, 63–67, 2002.

Nakamoto, K.: Infrared and Raman Spectra of Inorganic and Coordination Compounds, Wiley & Sons, New York, 1997.

Nishikawa, M., Kanamori, S., Kanamori, N., and Mizoguchi, T.: Kosa Aerosol as Eolian Carrier of Anthropogenic Material, Science of the Total Environment, 107, 13–27, 1991.

Pitts, J. N. J., Sanhueza, E., Atkinson, R., Carter, W. P. L., Winer, A. M., Harris, G. W., and Plum, C. N.: An investigation of the dark formation of nitrous acid in environmental chambers, International Journal of Chemical Kinetics, 16, 919–939, 1984.

Rognon, P., CoudeGaussen, G., Revel, M., Grousset, F. E., and Pedemay, P.: Holocene Saharan dust deposition on the Cape Verde islands: Sedimentological and Nd-Sr isotopic evidence, Sedimentology, 43, 359–366, 1996.

Sakamaki, F., Hatakeyama, S., and Akimoto, H.: Formation of nitrous acid and nitric oxide in the heterogeneous dark reaction of nitrogen dioxide and water vapour in a smog chamber, International Journal of Chemical Kinetics, 15, 1013–1029, 1983.

Schoonheydt, R. A. and Lunsford, J. H.: Infrared Spectroscopic Investigation of the Adsorption and Reactions of SO_2 and MgO, Journal of Catalysis, 26, 261–271, 1972.

Svensson, R., Ljungstrom, E., and Lindqvist, O.: Kinetics of the Reaction between Nitrogen-

Dioxide and Water-Vapor, Atmospheric Environment, 21, 1529–1539, 1987.
Tabor, K., Gutzwiller, L., and Rossi, M. J.: Heterogeneous Chemical-Kinetics of NO_2 on Amorphous-Carbon at Ambient-Temperature, Journal of Physical Chemistry, 98, 6172–6186, 1994.
Tegen, I. and Fung, I.: Modeling of Mineral Dust in the Atmosphere – Sources, Transport, and Optical-Thickness, Journal of Geophysical Research Atmospheres, 99, 22 897–22 914, 1994.
Tsyganenko, A. A. and Mardilovich, P. P., Structure of alumina surfaces, Journal of the Chemical Society-Faraday Transactions, 92, 4843–4852, 1996.
Ullerstam, M., Vogt, R., Langer, S., and Ljungstrom, E.: The kinetics and mechanism of SO_2 oxidation by O_3 on mineral dust, Physical Chemistry Chemical Physics, 4, 4694–4699, 2002.
Underwood, G. M., Li, P., Usher, C. R., and Grassian, V. H.: Determining accurate kinetic parameters of potentially important heterogeneous atmospheric reactions on solid particle surfaces with a Knudsen cell reactor, Journal of Physical Chemistry A, 104, 819–829, 2000.
Underwood, G. M., Miller, T. M., and Grassian, V. H.: Transmission FT-IR and Knudsen cell study of the heterogeneous reactivity of gaseous nitrogen dioxide on mineral oxide particles, Journal of Physical Chemistry A, 103, 6184–6190, 1999.
Underwood, G. M., Song, C. H., Phadnis, M., Carmichael, G. R., and Grassian, V. H.: Heterogeneous reactions of NO_2 and HNO_3 on oxides and mineral dust: A combined laboratory and modeling study, Journal of Geophysical Research Atmospheres, 106, 18 055–18 066, 2001.
Usher, C. R., Al-Hosney, H., Carlos-Cuellar, S., and Grassian, V. H.: A laboratory study of the heterogeneous uptake and oxidation of sulfur dioxide on mineral dust particles, Journal of Geophysical Research Atmospheres, 107, 4713, doi:10.1029/2002JD002051, 2002.
Zhang, D. Z., Shi, G. Y., Iwasaka, Y., and Hu, M.: Mixture of sulfate and nitrate in coastal atmospheric aerosols: individual particle studies in Qingdao (36°04′ N, 120°21′ E), China, Atmospheric Environment, 34, 2669–2679, 2000.
Zhang, Y. and Carmichael, G. R.: The role of mineral aerosol in tropospheric chemistry in East Asia – A model study, Journal of Applied Meteorology, 38, 353–366, 1999.
Zhang, Y. H. and Chan, C. K.: Understanding the hygroscopic properties of supersaturated droplets of metal and ammonium sulfate solutions using raman spectroscopy, Journal of Physical Chemistry A, 106, 285–292, 2002.

Table 1. Knudsen reactor parameters

Knudsen reactor parameter	
reactor volume, V	$3,72 \pm 0.03\,dm^3$
experimental temperature, T_{exp}	$299 \pm 0.2\,K$
escape orifice (pulsed flow), ϕ	11 mm
escape orifice (steady state flow), ϕ	2 mm
geometric sample area, A_{geo}	$33.2\,cm^2$

Table 2. Reactive uptake coefficients and other experimental data for the reaction of SO_2 and NO_2 with mineral dust at 299 K. BET surface area, 5.0×10^5 ($cm^2\ g^{-1}$)

$[SO_2]$ molecule cm^{-3}	$[NO_2]$ molecule cm^{-3}	$\gamma(SO_2)$ geometric	$\gamma(SO_2)$ BET	$\gamma(NO_2)$ Geometric	$\gamma(NO_2)$ BET
$(2.6 - 87) \times 10^{11}$	9.8×10^{12}	[a] $(1.5 \pm 0.6) \times 10^{-3}$	[a] $(5.7 \pm 1.9) \times 10^{-6}$	–	—
$(5.4 - 15) \times 10^{12}$	–	[a] $(1.3 \pm 0.3) \times 10^{-3}$	[a] $(4.6 \pm 0.3) \times 10^{-6}$	–	–
5.3×10^{12}	$(1.7 - 10) \times 10^{12}$	–	–	[a] $(2.0 \pm 0.4) \times 10^{-4}$	[a] $(6.3 \pm 1.0) \times 10^{-7}$
–	$(1.0 - 1.5) \times 10^{13}$	–	–	[a] $(1.9 \pm 0.4) \times 10^{-4}$	[a] $(6.2 \pm 3.4) \times 10^{-7}$
$(1.4 - 9.3) \times 10^{12}$	2.4×10^{13}	[b] $(1.6 \pm 0.6) \times 10^{-6}$	[b] $(2.6 \pm 1.1) \times 10^{-10}$		

[a] Knudsen experiment.
[b] DRIFTS experiments.

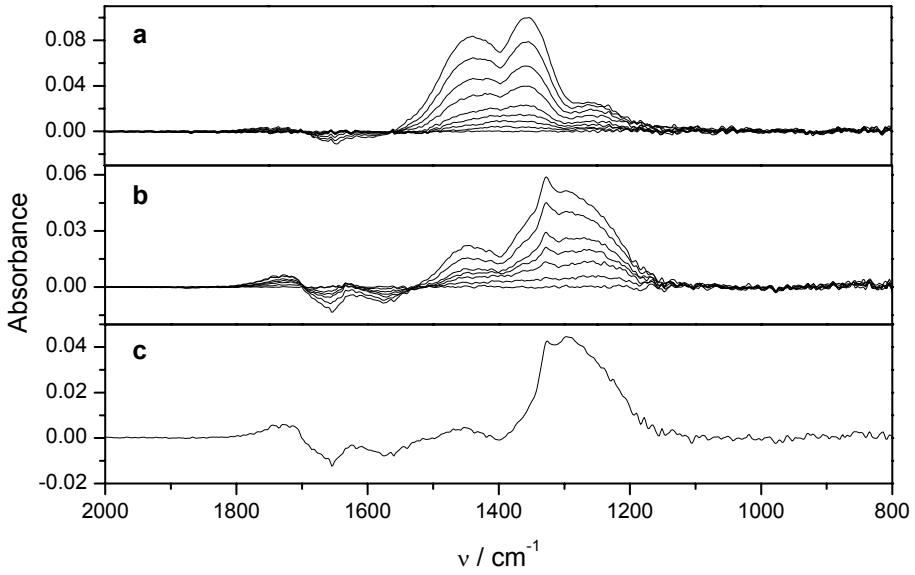

Fig. 1. Absorption difference spectra recorded during the reaction of mineral dust with SO_2 and NO_2. **(a)** experiment where the surface is exposed to NO_2 only ($[NO_2] = 2.2 \times 10^{13}$ molecule cm^{-3}). **(b)** experiment with exposure of both SO_2 and NO_2 ($[SO_2] = 9.4 \times 10^{12}$ and $[NO_2] = 2.5 \times 10^{13}$ in molecule cm^{-3}). **(c)** residue from subtraction of reference spectrum (a) from the final spectra of (b).

ACPD
3, 4069–4096, 2003

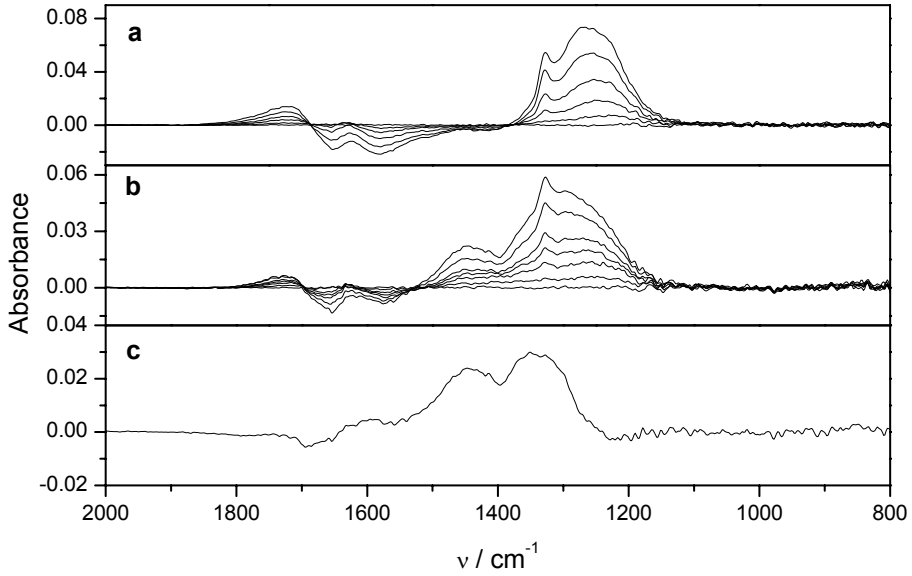

Fig. 2. Absorption difference spectra recorded during the reaction of mineral dust with SO_2 and NO_2. **(a)** reference spectra of sulfur species from reaction of SO_2 on mineral dust in the presence of O_3 (Ullerstam et al., 2002). **(b)** experiment with exposure of both SO_2 and NO_2 ($[SO_2] = 9.4 \times 10^{12}$ and $[NO_2] = 2.5 \times 10^{13}$ in molecule cm^{-3}). **(c)** residue from subtraction of reference spectrum (a) from the final spectrum of (b).

ACPD
3, 4069–4096, 2003

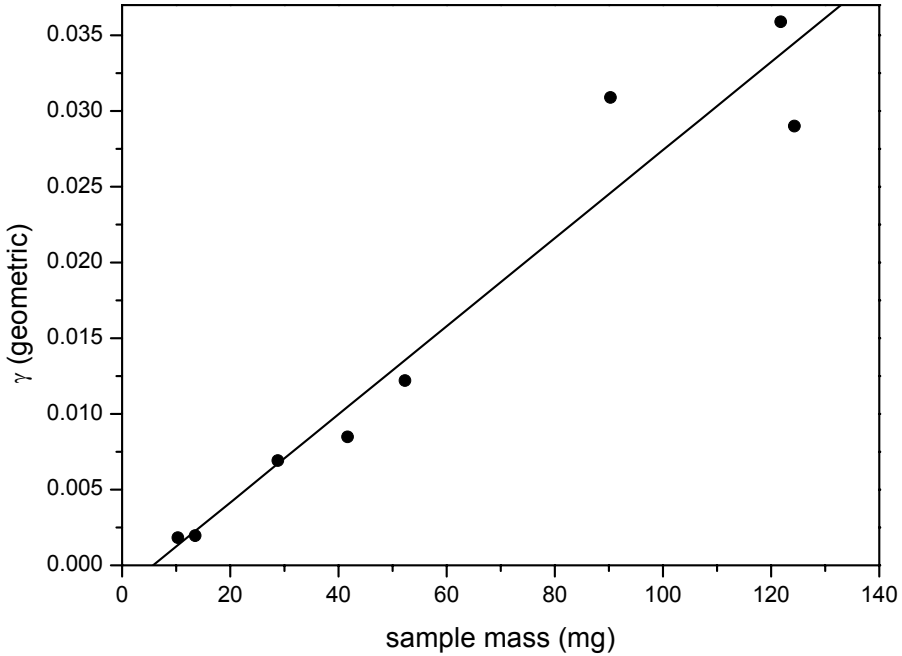

Fig. 3. Total uptake coefficient for SO_2 calculated using the geometric surface area as the effective surface area as a function of sample mass. Experiments were performed with a pulsed flow of SO_2 and NO_2. Initial concentrations of SO_2 and NO_2 were 2.7×10^{11} and 1.7×10^{11} molecules cm^{-3}, respectively.

ACPD
3, 4069–4096, 2003

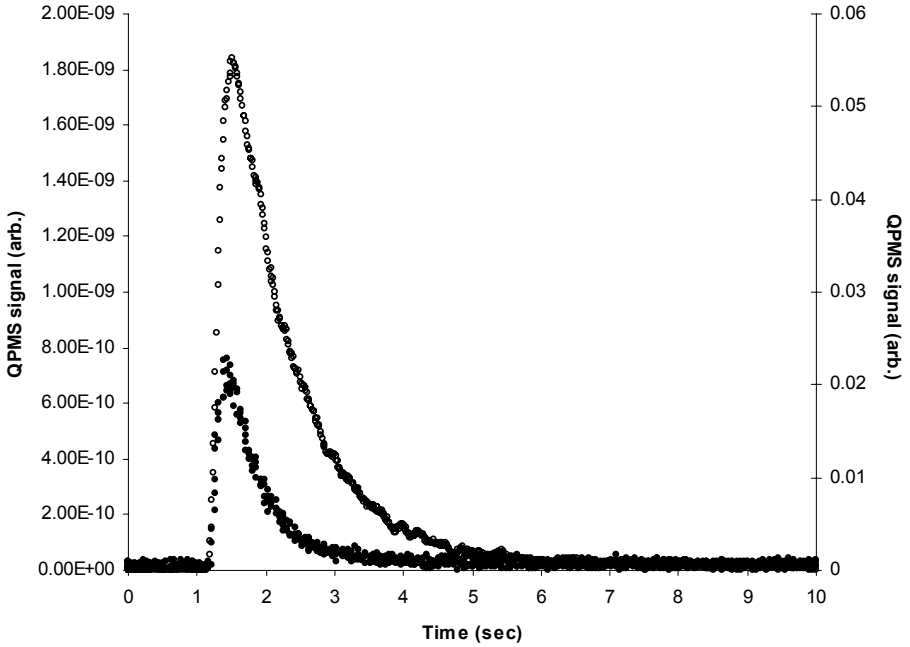

Fig. 4. An example of a typical Knudsen experiment performed with a pulsed flow showing the decay of the SO_2 signal (m/z = 64). Initial concentrations of SO_2 and NO_2 were 2.7×10^{11} and 1.7×10^{11} in molecules cm^{-3}, respectively. Empty circles represent the decay of SO_2 signal when the surface is covered, see right y-axis. Filled circles represent the decay of SO_2 signal during exposure of the sample surface, see left y-axis.

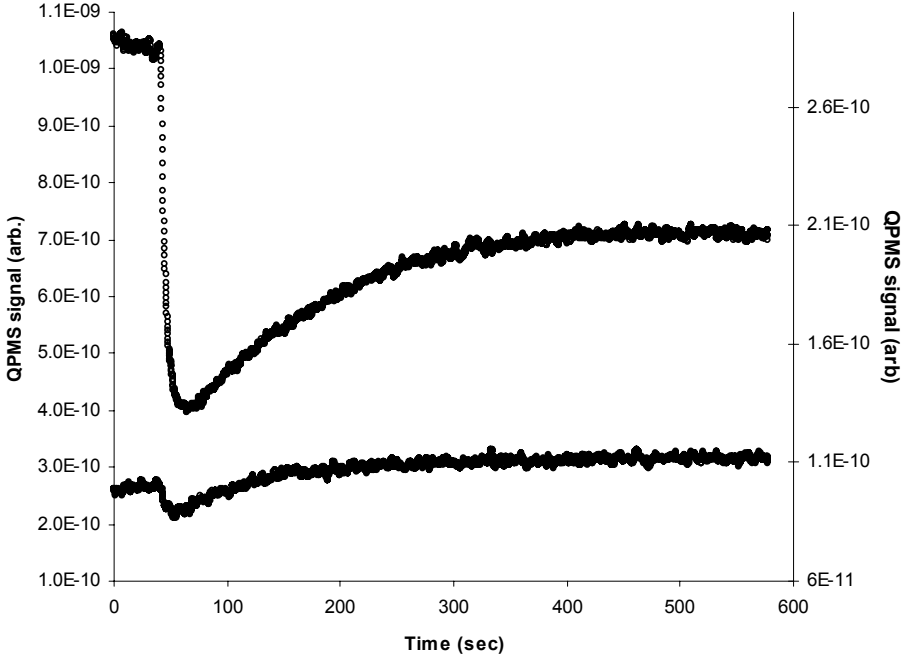

Fig. 5. An example of a typical Knudsen experiment performed with a steady state flow. Steady state concentrations of SO_2 and NO_2 were 5.0×10^{12} and 1.0×10^{13} molecules cm^{-3}, respectively. The top line represents the signal for SO_2 (m/z = 64) and belong to the left y-axis. The lower line represents the signal for NO_2 (m/z = 46) and belong to the right y-axis.

ACPD
3, 4069–4096, 2003

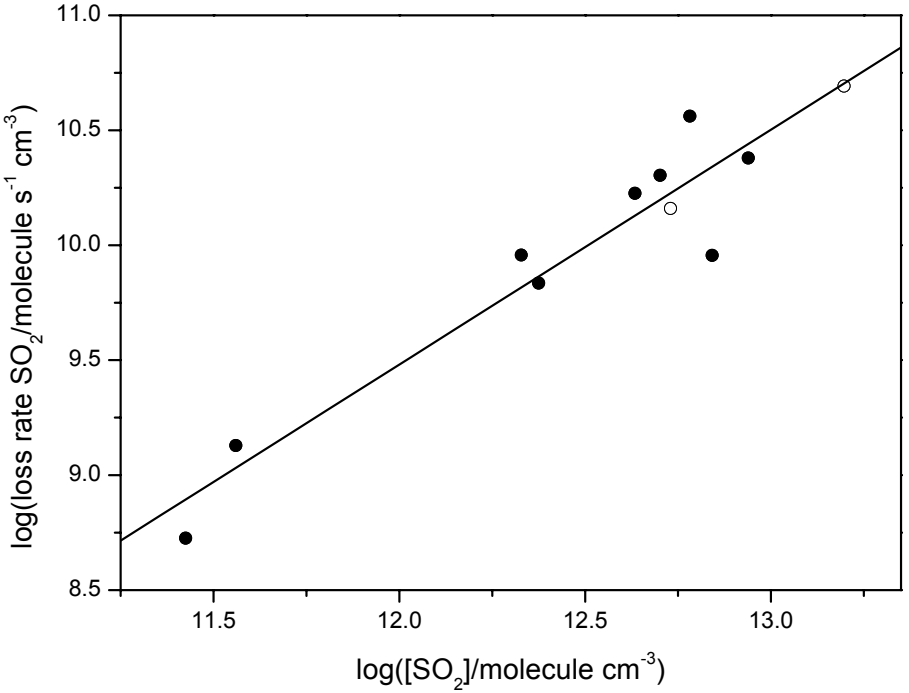

Fig. 6. A bilogarithmic plot of the loss rate of SO_2 as a function of $[SO_2]$. Filled circles are experiments with SO_2 and NO_2 present, open circles are from experiments with only SO_2 present. From linear regression of experiments with both SO_2 and NO_2 present (filled circles) the reaction order was determined to be $n = 1.01 \pm 0.15$ (2σ).

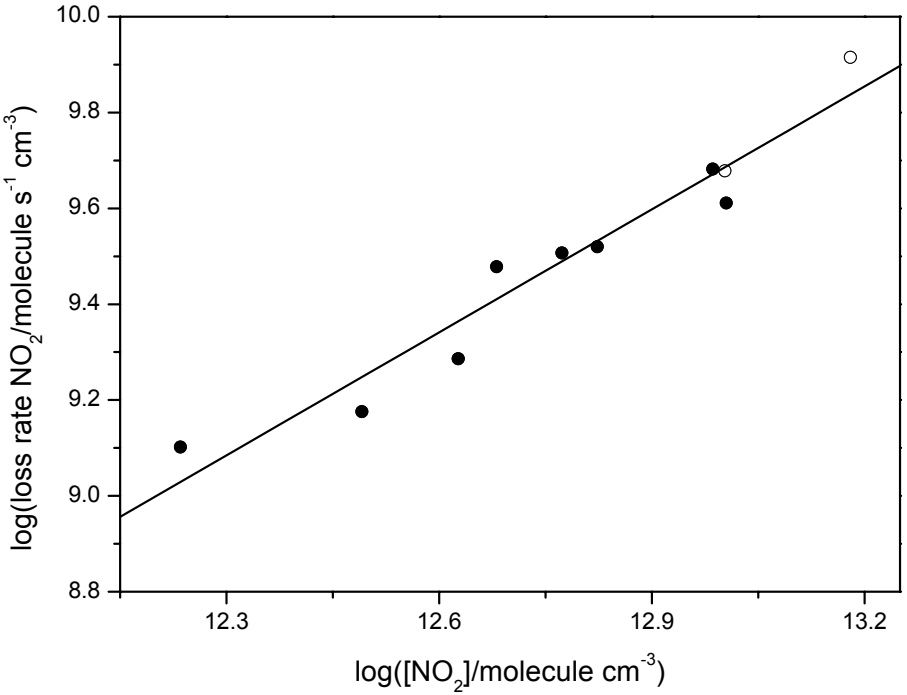

Fig. 7. Bilogarithmic plot of the loss rate of NO_2 as a function of $[NO_2]$. Filled circles are from experiments with both SO_2 and NO_2 present, open circles are from experiments with only NO_2. The reaction order was determined to be $n = 0.85 \pm 0.28$ (2σ) from linear regression of the experiments with SO_2 and NO_2 present (filled circles).

ACPD
3, 4069–4096, 2003

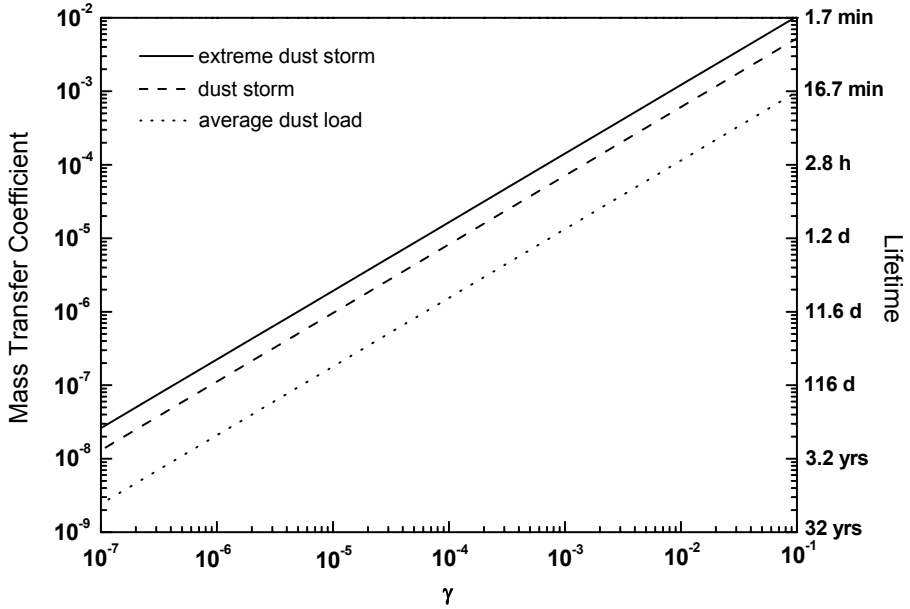

Fig. 8. Calculated mass transfer coefficients as a function of the heterogeneous uptake, γ, as described in the text Li et al. (2001). Data used for the calculations: Diffusion constant (D), 0.126 cm^2 s^{-1}, Lognormal distribution for mineral dust: N(average) = 798, N(storm) = 2800, N(extreme storm) = 5600; r, 0.88 μm; log(σ), 0.23; ρ_s = 2.0 μg m^{-3}. (Li et al., 2001; Zhang et al., 1999; Alpert et al., 2001).

ACPD
3, 4069–4096, 2003